Astronomical and Astrophysical Transactions (*AApTr*), 2019, Vol. 31, Issue 3, pp. 369–378,
ISSN 1055-6796, Photocopying permitted by license only, ©Cambridge Scientific Publishers

The study of the atmospheric turbulence structure for solar astronomy at the Baykal astrophysical observatory site

A.Yu. Shikhovtsev*, A.V. Kiselev, D.Yu. Kolobov, P.G. Kovadlo, I.V. Russkih, V.E. Tomin, M.Yu. Shikhovtsev

Institute of Solar-Terrestrial Physics, Siberian Branch, Russian Academy of Sciences, Irkutsk, Russia

Received 1 October, 2018

The present paper focuses on the study of the atmospheric turbulence at the Baykal astrophysical observatory site. An alternative method to Slodar technique is proposed for determining the heights of the atmospheric layers of intense atmospheric turbulence. The method is based on an estimation of the amplitudes of the time covariance between local slopes of the wavefront on the spaced subapertures in the field of view of the telescope for known angular displacement of the solar object due to the Sun's own motion. The estimates of the main heights of intense turbulence in the atmospheric boundary layer as well as the Fried radius at the BAO site are obtained.

Keywords: Atmospheric turbulence, Fried radius, profiling, telescope, adaptive optics system

1 Introduction

The Baykal Astrophysical Observatory (BAO; $51^\circ\,50'\,47''$ N, $104^\circ\,53'\,30''$ E) of the Institute of Solar-Terrestrial Physics is located at a height of 180 m above Baykal level in specific astrometeorological conditions. Turbulence is particularly suppressed in the lower atmospheric layer in the summer because of the stabilizing impact of cold water on the adjoining air. This effect improves the quality of astronomical images.

The primary instrument of BAO is the Large Solar Vacuum Telescope (LSVT) equipped with a 1-m siderostat. Work on the design of the adaptive optics (AO) system which corrects turbulent distortions of the wavefront has been carried out on LSVT since 2000. Nowadays a multimirror visible AO system consisting of two circuits of correction of solar images is being tested (Antoshkin et al., 2017). It should be noted that the design of the AO system is a non-trivial task. Specificity of its solution is determined not only by the optical set-up of the telescope but also by the structural features of the turbulent atmosphere at the instrument site.

*Email: Ashikhovtsev@iszf.irk.ru

There are a number of famous models of the height distribution of atmospheric (optical) turbulence. Among them one may note the statistical models developed by Hufnagel and Valley (Hufnagel, 1974), Mironov (Gurvich, 1976), Masciadri (Masciadri, 1999), Trinquet and Vernin (Trinquet, 2006). The models describe the behavior of the mean intensity of turbulence (the structural characteristic of the air refraction index fluctuations C_n^2) with height. The models do not have universality and can serve as a basis for estimating the amplitudes of the structural characteristic of the air refraction index fluctuations at different heights. The height profile of mean $C_n^2(z)$ has been calculated for the BAO site (Kovadlo, 2016). It is shown that the atmospheric boundary layer makes a main contribution to wavefront distortions. The permanent atmospheric layer of high intensity of the atmospheric turbulence has been found at a height of 12 km. Also, time recurring atmospheric layers have been detected in conditions of calm at heights of 3 and 6 km above sea level.

2 The features of the design of solar adaptive optics system to correct images

Functioning classical adaptive optics systems are based on the determination of the wavefront in plane optically conjugated with the telescope pupil in a narrow field of view (FOV) – in so-called isoplanatic angle of the atmosphere. At the same time, the wavefront distortions can be generated by the layers at different heights lying from the aperture of the telescope up to ∼20 km and, thus, can vary significantly in the FOV. The main reason of "non-compensation" of wavefront distortions in the extended FOV (30′–120′) is turbulence of the upper atmospheric layers. The quality of the adaptation of solar images as well as Strehl ratio become worse when moving away from the optical axis of the wavefront sensor. The degree of decreasing quality depends on the height profile as well as intensity of atmospheric turbulence. Thus, the modern development of astronomical visible AO is related to the solution of the multivariate task of extending corrected FOV, at least, up to 60–120′.

The design of AO system for a solar telescope is associated with a number of difficulties. First of all, the AO system of the solar telescope should correct high-amplitude short-period phase distortions in conditions of intense daytime turbulence.

In addition to turbulent distortion AO system must determines the slopes of the wavefront induced by both atmospheric turbulence and instrumental factors.

Moreover the AO system should operate with low-contrast, extended and time-varying solar objects in the visible wavelength range. For example, AO should be sensitive to the contrast of the "optical" images of 1–5% when determining the wavefront using solar granulation images. The mean contrast of the "optical" images of the solar granulation was observed by space instruments and varies from 9–14% (Roudier, 2017; Collados, 1987; Danilovic, 2008). The amplitude of these values is significantly reduced due to the influence of the earth's atmosphere (Lukin, 2016). Also, it may be noted that the contrast of speckle reconstructed images of solar granulation is higher (9%) than contrast of "optical" images obtained with (5 %) and, especially, long exposure (4%) (Denker, 2005). Due to low contrast of solar granulation images errors of assessment of local gradients of the wavefront increase. In particular, our experience of measurements of the higher-order aberrations by Shack–Hartmann sensor

has shown that the contrast of images must be higher than 2%. The contrast of the images also decreases due to the diffraction of light on the small size sub-apertures of the Shack–Hartmann sensor, each of which corresponds to a certain position on the aperture of the telescope.

Besides the contrast, the positional accuracy of determining local slopes of the wavefront from the centers of gravity of the sub-images focused by Shack–Hartmann sensor depends on the correspondence between the equivalent size of the subaperture, the coherence radius as well as the spatial scale of the observed objects on the Sun. Analysis of the spectra of the intensity shows that the spatial scales of the solar granulation vary over a wide range. However, typical sizes of smallest individual granules determined by the character of the changes of the power spectral density are equal to 2.5–0.6′ (Almeida, 2003).

Thus, the design of a new types of AO systems must be based on data on characteristics of the atmospheric turbulence including spectral composition of the optical distortions. The development of methods to reconstruct wavefront in a wide field of view is closely related to the character of the distribution of atmospheric turbulence with height. From this point of view the assessment of coherence of the wavefront as well as determination of the heights of intense atmospheric turbulence have formed the basis of the study.

3 The results of the measurements and estimation of the integral characteristics of the deformations of the wavefront at the BAO site

The development of AO system as well as new methods of correction of the wavefront in a wide FOV must be based on accounting spatial changes of the characteristics of the atmospheric turbulence at the selected site. In order to decide tasks related to the choice of the type and dynamic range of the AO system for LSVT as well as performance of AO elements, we have estimated the typical height profile of the structural characteristics of the air refraction index fluctuations as well as statistics: the effective velocity of turbulent flows, instrumental scale and effective outer scale of turbulence (Kovadlo, 2017; Lukin, 2012).

One of the key characteristics of turbulence is the Fried radius r_0, which characterizes spatial scale of "flatness" of the wavefront. This quantity determines the resolving power of the telescope β_0 in a turbulent atmosphere according to the formula (Fried, 1965):

$$\beta_0 = 0.98\frac{\lambda}{r_0}, \tag{1}$$

where λ is the wavelength of light.

The Fried radius is related to the dispersion of angles of light arrival σ_α^2 according to the relation (Tatarsky, 1967):

$$r_0 = \left(\frac{6.74 D_a^{-1/3}}{k^2\sigma_\alpha^2}\right)^{3/5}, \tag{2}$$

where D_a is the diameter of telescope aperture.

The physical basis for estimation of the Fried radius from differential measurements of the wavefront are described in detail in Botygina (2014). The Fried radius from measurements by the Shack–Hartmann sensor is determined by the formula (Botygina, 2014):

$$r_0 = 0.528 \left(\sigma^2_{\alpha 1-\alpha 2}\right)^{-3/5} \lambda^{6/5} D^{-1/5} \left(1 - 0.562(d/D)^{-1/3}\right)^{3/5}, \quad (3)$$

where D is the size of the subaperture, d is the distance between the centers of the subapertures, λ is the wavelength of light, $\sigma^2_{\alpha 1-\alpha 2}$ is the variance of the measured differences between local wavefront slopes toward aperture spacing.

Observations of image motion have been carried out in the first focal plane of the Large Solar Vacuum Telescope. The averaged values of the Fried radius at $\lambda = 0.5$ μm have been calculated using formula 2 for the period from 2008 to 2017. During this period, measurements of image motion were periodic. The values of dispersion of angles of light arrival σ^2_α have been averaged for 3 min time intervals. The total duration of continuous (no gaps) time series of image motion registered in different seasons is about 6 months. The probability of recurrence of the the daytime zenith values of the Fried radius for a wavelength of 0.5 μm is shown in Fig. 1.

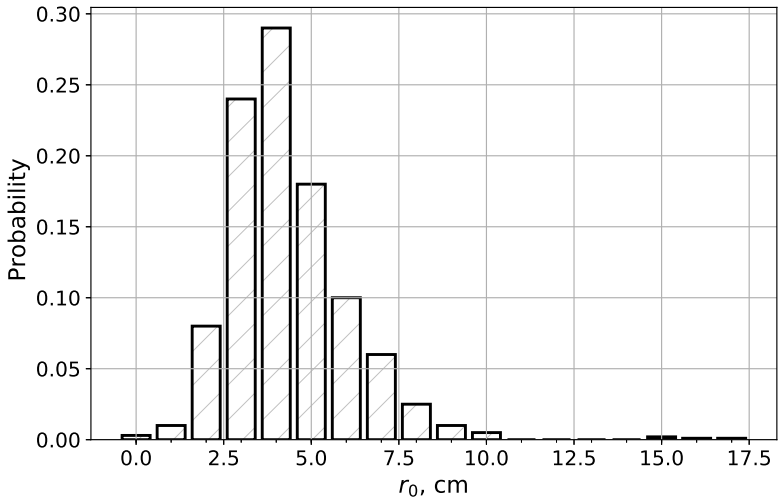


Figure 1 The probability of recurrence of the daytime zenith values of the Fried radius for a wavelength of 0.5 μm, LSVT site.

Analysis of the probability of recurrence of the daytime zenith values of the Fried radius points to a wide range of variations of coherence scale. Typically r_0 varies within range from 1 to 10 cm. The probability of recurrence of the best atmospheric astroclimatic conditions, in which it is possible to observe a so-called "Lucky images" is limited by a few percent.

To characterize the dynamics of the Fried radius on the short time interval from Shack–Hartmann sensor measurements we used relation 3. The Shack–Hartmann sensor is the component of the multimirror AO system (Antoshkin et al., 2017). The

values of the Fried radius have been estimated from measurement data of edge solar images motion obtained 28.06.2018. The variations of the daytime zenith values of the Fried radius and its extremes observed in the FOV calculated from measurements of Shack–Hartmann sensor are shown in Fig. 2.

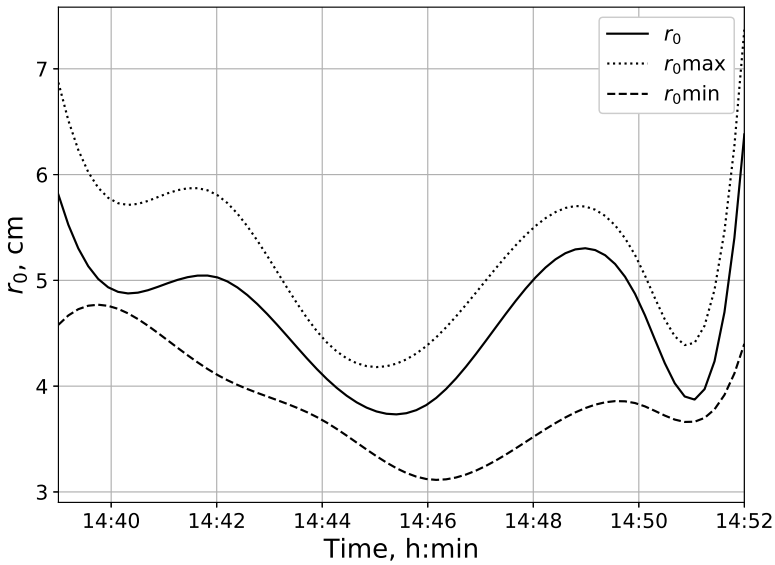


Figure 2 The variations of daytime zenith values of the Fried radius and its extremes observed in the FOV calculated from measurements of Shack–Hartmann sensor.

The time of observations is shown along the abscissa; the values of the Fried radius, along the ordinate. A continuous line shows the variations of the averaged values of the Fried radius estimated from the subimages motions using 52 neighboring pairs of the separated illuminated subapertures. Time variations of the minimal values of the Fried radius in the FOV of the wavefront sensor are shown by the dashed line. The maximal values of the Fried radius in the FOV are depicted by the dotted lines.

The analysis of the coherence of the wavefront indicates to significant amplitudes of the variations both in time and in the field of view. One may observe large size coherent regions (equivalent to the Fried radius ∼7 cm and more) in a rather narrow field of view as well as in short time intervals under moderate quality of solar images.

4 The wavefront distortions induced by the height distribution of the turbulent characteristics

In real time, the height profiles of the atmospheric turbulence are often recovered with the help of remote methods: S DIMM+ and Slodar (Osborn, 2017; Blary, 2004; Wilson, 2002; Nosov, 2012; Nosov, 2016).

The S DIMM+ method is based on the analysis of the differential motion of subimages on spaced subapertures. The essence of this method is the estimation

of the covariance of differences of the differential motion of images of a few objects spaced at an angle:

$$C_*(i,j) = \langle \delta x_1 \cdot \delta x_2 \rangle, \tag{4}$$

$$\delta x_1(i,0) = \sum_{i=1}^{n} s_n(i) - s_n(0), \tag{5}$$

$$\delta x_2(i,\beta) = \sum_{i=1}^{n} s_n(i+\beta z_n) - s_n(\beta z_n). \tag{6}$$

Indices 1 and 2 correspond to light sources (granules, sun spots, pores), z_n is the height of the turbulent layer n, $s_n(0)$ – wavefront slope induced by the turbulent layer n on reference subaperture, i – index of the subaperture, β – angle between "axial" and "non axial" objects within FOV of a given subaperture. Analysis of covariances of differential motion is performed along one (typically) of the axes between the selected (reference) subaperture and subapertures space towards the periphery of FOV of the wavefront sensor. The distance of spacing is proportional to δi in the plane conjugated with the aperture.

According to the Slodar method, the height profiles of the atmospheric turbulence may be recovered from time averaged cross-correlation functions of local slopes of the wavefront measured by the Shack–Hartmann sensor using the relationship:

$$C_s(\delta i, \delta j) = \frac{\left\langle \sum_{i=1,j=1}^{i=n,j=m} s_{i,j}^{[1]} s_{i+\delta i, j+\delta j}^{[2]} \right\rangle}{O(\delta i, \delta j)}, \tag{7}$$

where i, j are indices of the subapertures, t is time, $s_{i,j}^{[1]}$ – local slopes of the wavefront on the subaperture i, j of the first camera [1], $s_{i+\delta i, j+\delta j}^{[2]}$ – local slopes of the wavefront on the subaperture $i+\delta i, j+\delta j$ of the second camera [2], $O(\delta i, \delta j)$ – the number of crossed illuminated subapertures. The height resolution of the Slodar method is about the same as for the S-Dimm+. The heights may be determined in accordance with the ratio:

$$z = \frac{D}{n\theta} \cdot \cos\alpha, \tag{8}$$

where D – diameter of aperture, n – the number of apertures, θ – angle between objects observed, α – zenith angle. Using these methods based on triangulation of light beams allows us to estimate effects of turbulence of atmospheric layers on wavefront structure within a given FOV (Blary, 2004; Nosov, 2012; Osborn, 2017; Wilson, 2002).

Taking into account the approach of "triangulation" of the Slodar and S-Dimm+ techniques the essence of our method is based on the estimation of time averaged covariances between wavefront local slopes on spaced subapertures in the field of view of the telescope. Analysis of local slopes on the spaced subapertures carried out taking into account the fact that the angular displacement of solar object due to own motion of the Sun is known. Taking into account angular displacement which depends on δt we can improve the approach based on (7):

$$s_{i,j}^{[1]} = s_{i,j}(t), \tag{9}$$

Considering that the structure of the atmospheric turbulence changes little over time δt local slopes at the spaced subaperture may be represented as:

$$s_{i+\delta i,j+\delta j}^{[2]} \sim s_{i+\delta i,j+\delta j}(t+\delta t). \tag{10}$$

It is possible to assess the angular shift between the primary position of the light beam (at time t) and the current position (at time $t+\delta t$) from frame to frame knowing the changes of zenith and azimuth angles during the measurements of the wavefront. The angular displacement of an observed solar object in time is approximately 15 arc sec/sec and gives us a possibility to analyze the synchronization between reference (for $t = 0$) and spaced wavefronts (for $t = \delta t$).

The height profile of the atmospheric turbulence (expressed in relative units) will be determined by the shape of covariance curve:

$$C(\delta t, \delta i, \delta j) = \frac{\langle \sum_{i=1,j=1}^{i=n,j=m} s_{i,j}(t) s_{i+\delta i,j+\delta j}(t+\delta t) \rangle}{O(\delta i, \delta j)}, \tag{11}$$

where $s_{i,j}(t)$ – local slopes of the wavefront on the reference subaperture, $s_{i+\delta i,j+\delta j}(t+\delta t)$ – local slopes of the wavefront on the supapertures spaced from reference one, δt – time shift, for which the coefficient of covariance is estimated. Averaging is performed over time and for the array of the subapertures. The height resolution of this method (in comparison with eq. 12) increases and is determined as:

$$z = \frac{D}{n\theta(\delta t)} \cdot \cos\alpha. \tag{12}$$

In practice, the height resolution is limited by the frequency range of the wavefront sensor. Thus, the method is based on covariance of the local spaced slopes of the wavefront shifted in time.

The proposed method based on estimating $C(\delta t, \delta i, \delta j)$ using (11) allows us to determine the heights of intensive atmospheric turbulence.

The height profiles of $C(\delta t, \delta i, \delta j)$ have been calculated at the Large Solar Vacuum Telescope site of the BAO using data of the measurements of the local slopes of the wavefront. The examples of the height profiles of $C(\delta t, \delta i, \delta j)$, LSVT calculated 28.06.2018 are shown in Fig. 3. Averaging of covariances is performed over time intervals of ∼2–3 min. Heights are plotted along the abscissa, zenith values of C $(\delta t, \delta i, \delta j)$ – along the ordinate.

Analysis of Fig. 3 shows that $C(\delta t, \delta i, \delta j)$ is distributed unevenly with height. The greatest variability of $C(\delta t, \delta i, \delta j)$ is observed in the lower layers of the atmosphere. Peaks of the covariances are observed at heights of 230, 650 and 1050 m. The calculated profiles of $C(\delta t, \delta i, \delta j)$ for different time intervals indicate a high repeatability of (i) the height position of the atmospheric layer of intense atmospheric turbulence in the range from 600 to 900 m and (ii) the developed turbulence in the lower layers of the atmosphere.

Also, the pattern of the height distribution of atmospheric turbulence is consistent with the obtained data of lidar observations of the vertical structure of air flows (Banakh, 2016). Experimental studies of the atmosphere performed with the help of

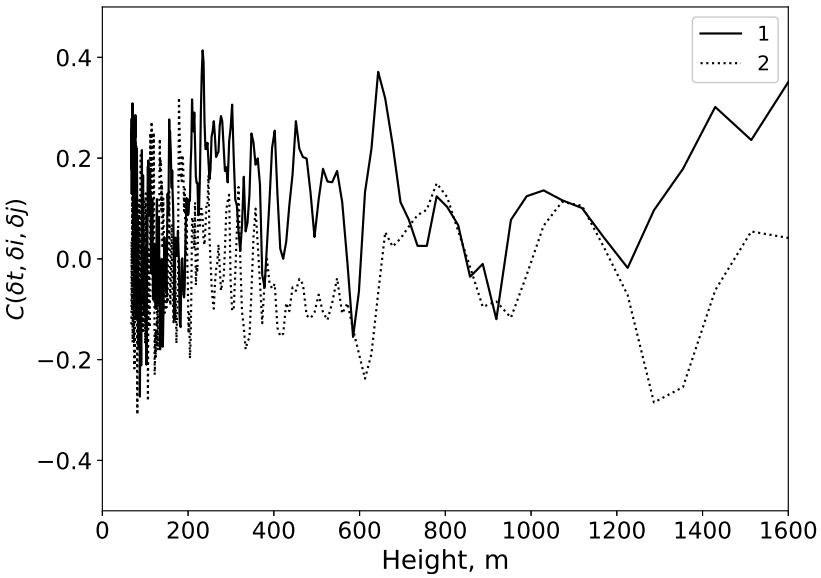


Figure 3 Height profiles of $C(\delta t, \delta i, \delta j)$, LSVT. Line 1 indicates the height profile of $C(\delta t, \delta i, \delta j)$ at 14:41; line 2, at 14:42.

Stream Line lidar revealed the structural features of the atmospheric boundary layer at the BAO site (Banakh, 2017). The complex character of changes of wind speed and direction with height was confirmed. As a rule, low level jet streams are observed at heights of 150–250 m and 500–800 m at the Large Solar Vacuum Telescope site.

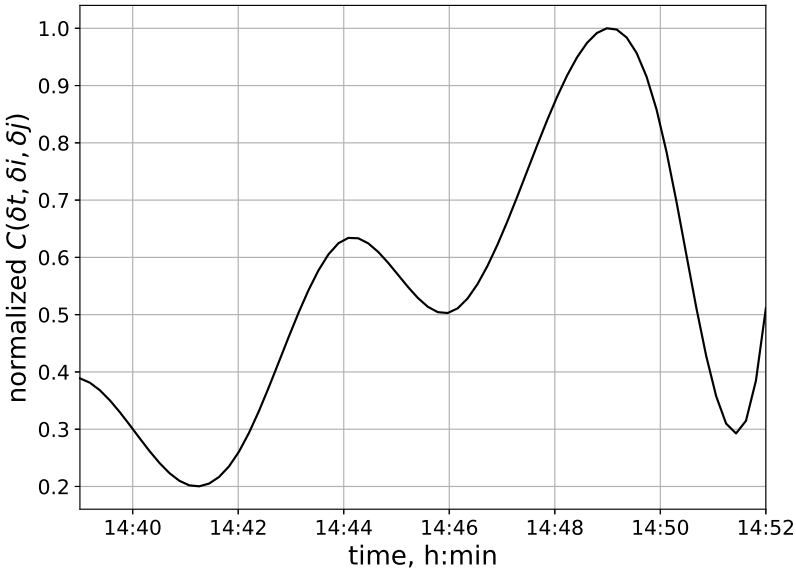


Figure 4 Daytime changes of normalized $C(\delta t, \delta i, \delta j)$, LSVT.

The estimates of the heights of intensive atmospheric turbulence obtained from measurements are consistent with typical heights of high values of wind speed (Banakh, 2016). In order to verify the method we have used the quantity k which is proportional integral value of $C(\delta t, \delta i, \delta j)$ in the atmospheric layer from 0 to 1500 m:

$$k = \frac{\int\limits_{z_1}^{z_2} C(\delta t, \delta i, \delta j)\, dz}{(\int\limits_{z_1}^{z_2} C(\delta t, \delta i, \delta j)\, dz)_{max}}, \tag{13}$$

where $(\int\limits_{z_1}^{z_2} C(\delta t, \delta i, \delta j)\, dz)_{max}$ is the maximum value of the integral characteristic k in the time series, $z_1 = 0$ m, $z_2 = 1500$ m. The characteristic k has been estimated for each time realization of local slopes of the wavefront. Daytime changes of normalized $C(\delta t, \delta i, \delta j)$ characterizing the integral intensity of atmospheric turbulence in the layer from 0 to 1500 m are shown in Fig. 4. Analysis of Figs 4 and 2 shows that the obtained values of k vary synchronously with the Fried radius estimated in the layer from 0 to a height of about 20 km. The values of the Fried radius estimated in the layer from 0 to 20 km tend to decrease with increasing averaged values of k and vice versa. Thus, we can conclude that synchronization between changes of k and r_0 indicate proportionality of the covariances to intensity of the atmospheric turbulence.

Conclusion

The paper points to modern problems in the development of solar adaptive optics systems. The performance of adaptive optics is determined not only by the integral intensity but also by the height distribution of turbulence along the line of sight. A new method to determine the heights of the atmospheric layers of intense atmospheric turbulence is proposed. The Slodar technique has been used as the basis for construction of the method. The essence of the method is the estimation of time synchronization between local slopes of the wavefront on the reference subaperture and local slopes of the wavefront shifted in time on the spaced subapertures. Analysis of the wavefront shifted in time allowed us to improve the method of crossing of the optical beams for recovery of the turbulence profiles. According to this method the height of the atmospheric layer is determined by the angular displacement of the observed solar light source which is about $15'$/sec and the distance between the considered subapertures. It is shown that the variations of the integral covariances between shifted in time local slopes of the wavefront on the reference and spaced subapertures is inversely proportional to changes of the Fried radius. The main heights of intense atmospheric turbulence in the atmospheric boundary layer at the BAO site are located at 230, 650 and 1050 m. Previously obtained data (Kovadlo, 2016) as well as the character of changes of the Fried radius will be used to obtain amplitudes of the structural characteristics of the atmospheric turbulence at the different heights.

The results obtained can serve as the basis for the development of multimirror systems of AO raising the resolving power of the telescope in a wide FOV.

Acknowledgements

The results were obtained using the Unique Research Facility Large Solar Vacuum telescope http://ckp-rf.ru/usu/200615/. The reported study was funded by RFBR according to the research project No 18-35-00033. The analysis of adaptive optics was supported by RSF 19-79-00061.

References

Almeida J.S. 2003, Astronomy & Astrophysics, V. 4629, p. 7.
Antoshkin L.V. et al. 2017, Atmospheric and Oceanic Optics, V. 30, 291.
Banakh V.A., Smalikho I.N. 2016, Atmos. Meas. Tech., V. 9, p. 5239.
Banakh V., Smalikho I., Fatits A. 2017, Proc. SPIE, V. 104662, p. 7.
Blary F. et al. 2004, Proc. SPIE, V. 91453H, p.10.
Botygina et al. 2014, Atmospheric and Oceanic Optics, V. 27, 2, p. 142.
Collados M., Vazquez M. 1987, Astronomy and Astrophysics, V. 180 p. 223.
Danilovic S. et al. 2008, Astronomy and Astrophysics, V. 484, p. 5.
Denker C. et al. 2005, Solar Physics, V. 227 p. 217.
Fried D. L.1965, J. Opt. Soc. America A, V. 56 p. 1372.
Gurvich A.S. et al. 1976, M.: Nauka, p. 277.
Hafnaguel R.E. 1974, in The Infrared Handbook, USGPO, C. 6,p. 50.
Kovadlo P.G., Shikhovtsev A.Yu. 2016, Proc. SPIE, V. 10035, p. 5.
Kovadlo P.G. et al. 2017, Proc. SPIE, V. 10466, p. 5.
Lukin V.P., Nosov V.V., Nosov E.V., Torgaev A.V. 2016, Applied Optics, V. 55, 12, p. 163.
Lukin V.P., Botugina N.N., Emaleev O.N.,Antoshkin L.V., Konyaev P.A. 2012, Proc. SPIE. Adaptive Optics System. p. 84474A.
Masciadri E., Vernin J., Bougeault P. 1999, Astronomy and Astrophysics Supplement Series, V. 137, 1, p. 185–202.
Nosov V.V., Lukin V.P., Nosov E.V., Torgaev A.V. 2012, Atmospheric and Oceanic Optics, V. 30, I.2, p. 176.
Nosov V.V., Lukin V.P., Nosov E.V., Torgaev A.V. 2016, Russian Physics Journal, V. 59, I.12, p. 138.
Osborn J. 2017, Profiling the turbulent atmosphere and novel correction techniques for imaging and photometry in astronomy. Thesis presented for the degree of Doctor of Philosophy, p. 161.
Roudier Th., Malherbe J.M., Mirouh G.M. 2017, Astronomy and Astrophysics, V. 598, p. 7.
Wilson R.W. 2002, Mon. Not. R. Astron. Soc., V. 337, p. 103.
Trinquet H., Vernin J. 2002, P. Astronomical Soc. Pacific, V. 118, 843, p. 756.